

Predicting Sleeping Disorders After mTBI: A Role for Inflammation and Brain Network Biomarkers

Rui Du^{1,*}, Yue Yu^{1-4,*}, Xiwen Zhu², Ranchao Wang¹, Yu Yang¹, Yang Li¹, Subo Zhang³, Hui Su⁴

¹Department of Radiology, Zhenjiang First People's Hospital, Zhenjiang, Jiangsu, People's Republic of China; ²Department of Surgery, Lishui People's Hospital, Nanjing, Jiangsu, People's Republic of China; ³Department of Radiology, The Second People's Hospital of Lianyungang, Lianyungang, Jiangsu, People's Republic of China; ⁴Department of Radiology, Gaoyou People's Hospital, Yangzhou, Jiangsu, People's Republic of China

*These authors contributed equally to this work

Correspondence: Subo Zhang, Department of Radiology, The Second People's Hospital of Lianyungang, No. 41 Hailian East Road, Haizhou District, Lianyungang, Jiangsu, People's Republic of China, Tel +0518-85775003, Email zhangsubolyg@126.com; Hui Su, Department of Radiology, Gaoyou People's Hospital, No. 10, Dongyuan Road, Gaoyou, Jiangsu, People's Republic of China, Tel +86 18852869930, Email 18852869930@163.com

Purpose: To predict the occurrence of sleeping disorders (SD) in patients with mild traumatic brain injury (mTBI) 3 months after injury.

Methods: This study recruited a total of 232 patients with mTBI and underwent a three-month follow-up period. Demographic information, MRI images, and inflammatory factor levels were collected one month after injury and PSQI (Pittsburgh Sleep Quality Index) scores were collected three times respectively on admission, 1 month and 3 months after injury. These mTBI patients were divided into those with SD group (mTBI-SD, n=130) and without SD group (mTBI-ND, n=85) based on PSQI score three months after injury. Differential indicators were used to construct univariate and multivariate logistic regression models, and receiver operating characteristic (ROC) curves were plotted. Pearson correlation analysis was conducted to explore the relationship between the differential indicators and PSQI scores.

Results: Compared to the mTBI-ND group, patients in the mTBI-SD group exhibited lower levels of OLF.L nodal efficiency, ACG.L nodal efficiency, rich-club connection strength, and feeder connection strength, as well as higher levels of IL-8, IL-10, and TNF- α . In the univariate logistic regression model, OLF.L, ACG.L, rich-club connection strength, IL-8, and TNF- α were identified as risk factors for the occurrence of SD three months after injury. Their Area Under the Curve (AUC) values were 0.669, 0.589, 0.672, 0.649, and 0.709, respectively. Among them, OLF.L nodal efficiency (78.80%) and rich-club connection strength (76.50%) exhibited higher specificity, while TNF- α (73.82%) demonstrated higher sensitivity. According to the multivariate regression results, the combined model constructed had an ROC-AUC of 0.809, with an accuracy of 75.35%, a sensitivity of 74.62%, and a specificity of 76.47%. The correlation results indicate that OLF.L nodal efficiency, rich-club connection strength and TNF- α are significantly correlated with PSQI scores three months after injury ($r_{OLF.L} = -0.461$, $r_{rich-club} = -0.563$, $r_{TNF-\alpha} = 0.538$).

Conclusion: The logistic regression model and ROC curve based on OLF.L nodal efficiency, rich-club connection strength and TNF- α can effectively predict the occurrence of SD in mTBI patients 3 months after injury.

Keywords: mild traumatic brain injury, sleeping disorders, white matter, graph theory, prediction

Introduction

Mild traumatic brain injury (mTBI) encompasses minor brain damage induced by external forces, commonly presenting as transient loss of consciousness, headaches, and cognitive impairments. The long-term ramifications may include notable alterations in neurological function and mental well-being.¹ Sleeping disorders (SD), the most prevalent sequelae after mTBI, are distinguished by their brief prodromal phase, high incidence, and a tendency towards neglect. These features frequently contribute to adverse prognoses in mTBI patients and may even precipitate the onset of other more severe disorders.^{2,3} Despite ongoing research endeavors aimed at constructing predictive models for sleep disturbances following mTBI, the predictive power of these models remains inadequate.

Recent advances in diffusion tensor imaging (DTI), which assesses white matter (WM) structural integrity by tracking water molecule diffusion, have established WM network topology as a novel paradigm in neuroscience. This approach models the brain as a structural network where cortical regions are defined as nodes and WM fiber bundles are defined as edges, elucidating principles of connectivity organization.⁴ Graph theory quantifies topological properties at global- and nodal-levels. Small-world properties belongs to global properties, while nodes of brain region show different characteristics by nodal efficiency and degree. Networks can be subdivided into three hierarchical subclasses based on the nodal degree: rich-club connections (strongest hub-to-hub links enabling global integration), feeder connections (moderate hub-to-non-hub links), and local connections (weak non-hub links maintaining regional segregation).⁵ This framework balances macroscopic network features (eg, efficiency) and microscopic behavioral correlates, with applications extending to robustness analysis in social networks.^{6,7} However, while DTI-based studies reveal altered WM topology in mTBI-SD,^{8–10} structural networks offer limited predictive power for dynamic progression. DTI provides static, macro-scale snapshots of WM integrity but fails to capture latent pathological dynamics. Thus, identifying trajectory-sensitive biomarkers remains critical to characterize WM degeneration mechanisms in mTBI-SD.

The complexity of mTBI lies not only in acute-phase mechanical damage but also in persistent biological injury mechanisms during the chronic phase. Studies reveal that inflammatory cytokines such as IL-8, IL-9, IL-10, IL-17A, MCP-1, and TNF- α remain significantly elevated in mTBI patients up to one year post-injury.¹¹ These cytokines drive white matter pathology by activating neuroinflammation, inducing oligodendrocyte apoptosis, and disrupting the blood-brain barrier, ultimately leading to white matter demyelination and axonal dysfunction.¹² For instance, TNF- α inhibits the differentiation of oligodendrocyte precursor cells critical for myelin repair, while elevated IL-8 levels correlate directly with DTI-derived parameter deterioration in key white matter tracts like the corpus callosum.¹³ This chronic inflammatory state persistently disrupts neuron-glia network functionality, causing hallmark cognitive impairments such as slowed information processing, thereby serving as a central driver of long-term mTBI sequelae.¹⁴ Unlike acute-phase white matter injury, which is modulated by multi-stress interactions (eg, mechanical compression and systemic stress responses), chronic-phase inflammatory factors (eg, IL-8, MCP-1) dominate progressive white matter degeneration and exhibit predictive power for disease progression.^{15,16} To address the limitations of relying solely on static structural network metrics (eg, DTI-based connectivity), integrating inflammatory biomarkers (dynamic indicators of pathological trajectories) with white matter network parameters (static markers of regional integration, such as rich-club connectivity) offers a multimodal approach to enhance predictive accuracy for SD. This strategy not only advances mechanistic insights into chronic injury pathways but also identifies novel therapeutic targets for neuroinflammation, bridging gaps in conventional structural network analyses.

To mitigate the impact of lesions on DTI data analysis and the unstable fluctuations in inflammatory factors levels during the acute phase, based on the feasibility of the 3-month model analysis proposed by Suzana Djukic and Joy Noelle Yumul,^{17–19} this study, for the first time, explores the potential correlation between the levels of two parameters at 1 month after injury and the occurrence of SD 3 months after injury. It evaluates their individual and combined predictive value and analyzes the relationship between the topology of inflammatory factors and WM structural network and clinically relevant indicators of SD. The findings of this study aim to provide a basis for guiding the clinical diagnosis, treatment, and prevention of mTBI-SD.

Method

Guided by the latest version of the Helsinki Declaration, this study was approved by the Ethics Committee of Zhenjiang First People's Hospital. All participants provided written consent after receiving a complete and detailed description of the study.

Participants

The study recruited patients with first-episode traumatic brain injury (TBI) who visited the outpatient or emergency departments of Zhenjiang First People's Hospital between January 2021 and June 2022. The inclusion criteria were as follows: (1) The Glasgow Coma Scale (GCS) score ≥ 13 at admission,² Marshall CT classification of Grade I or II, and duration of coma < 30 minutes;²⁰ (2) Age between 18 and 40 years, regardless of gender; (3) Daytime workers. The

exclusion criteria included: (1) History of previous brain injury; (2) History of psychotic symptoms caused by medication or organic diseases; (3) History of other previous or current diseases affecting brain function and structure (eg Depression Parkinson's, anxiety, PTSD, etc); (4) History of sleeping disorders (PSQI score ≥ 8) or history of using sleep-related medications;¹⁹ (5) Presence of MRI contraindications (eg cardiac pacemaker, artificial valve replacement, ferromagnetic vascular clips, metallic foreign bodies in the eyeball, high fever, pregnant within the first three months of pregnancy). All subjects were followed up at 1 month and 3 months after injury.

Ultimately, a total of 232 patients with first-episode mild TBI (mTBI) who met the inclusion and exclusion criteria were enrolled. Baseline data were collected from these 232 subjects, including age, gender, BMI, cause of mTBI, smoking, alcohol, previous PSQI scores before injury, GCS scores at admission, and Marshall CT classification, and were recorded for analysis. To avoid the acute abnormalities of numerous biomarkers in the short period after injury and the errors introduced by intracranial hematoma in brain network analysis (which differ from the stable state in the subacute and chronic phases), we chose to collect inflammatory cytokine levels and conduct brain DTI data scans one month after injury. This approach also avoided the differences in mTBI interventions across different medical environments and individual differences in recovery capacity. Three months after injury, all subjects were assessed for sleep quality via telephone or email. During the follow-up period, 17 subjects were excluded, including 4 with secondary injuries, 4 who took medication on their own, 6 who were lost to follow-up, and 3 whose image showed the bad MRI data quality. Therefore, the final number of mTBI patients included in the study was 215.

Based on whether the PSQI score 3 months after injury was more than or equal to 8, the 215 subjects were divided into two groups: the mTBI-SD group (130 subjects with sleeping disorders after mild traumatic brain injury) and the mTBI-ND group (85 subjects without sleeping disorders after mild traumatic brain injury). Specifically, the PSQI score in the mTBI-SD group was ≥ 8 .

Measure and Evaluation

Assessment of Sleep Quality

All patients and normal controls were taken the PSQI test to assess their sleeping quality and future diagnose of SD. PSQI is a tool employed to evaluate sleep quality over the preceding month. It encompasses 19 items across seven categories: subjective sleep quality, sleep latency, sleep duration, habitual sleep efficiency, sleep disturbances, use of sleeping medications, and daytime dysfunction, with each item scored between 0 and 3. The cumulative PSQI ranges from 0 to 21, where higher scores signify poorer sleep quality. Generally, scores exceeding 5 are regarded as indicative of poor self-reported sleep quality.¹⁹

Diffusion MRI Acquisition and Preprocessing

All patients and normal controls underwent magnetic resonance (MR) scanning one month after injury using a 3.0 Tesla Siemens Tim Trio MRI scanner equipped with an 8-channel head coil. During the scan, subjects were placed in the supine position with their heads fixed, remaining awake and with their eyes closed. Padding and headphones were used to minimize head movement and scanner noise. The procedure began with three-plane localization, followed by axial T1-weighted imaging (T1WI) with the following parameters: repetition time (TR)/echo time (TE) = 580 ms/18 ms, T1 = 2400 ms, field of view (FOV) = 240 mm, slice thickness = 5 mm, slice gap = 1 mm, and 20 slices acquired in total, covering the entire brain. After completion, structural images were visually and rapidly screened by a radiologist with 10 years of experience to initially exclude cases with obvious intracranial organic lesions (none were found in this study). Following the routine three-plane localization, diffusion-weighted echo-planar imaging (DW-EPI) was employed for oblique-axial diffusion tensor imaging (DTI) scanning with the anterior and posterior commissural line as the scanning baseline. Scanning parameters were: TR = 10,000 ms, TE = 76 ms, FOV = 320 mm, matrix = 128×128, number of excitations (NEX) = 1. The scanning range was from the vertex to the foramen magnum, with a slice thickness of 2.5 mm, no gap, and 60 slices acquired in total. Diffusion-sensitizing gradients were applied along 64 different nonlinear directions at b-values of 0 and 1000 s/mm². The raw DTI image files were transferred from the MR scanner to a computer and saved using an eFilm workstation. All MR image

acquisitions were performed by trained and dedicated technicians on the same MR scanner. T1-weighted and DTI data were collected for all participants.

The preprocessing of DTI data involves data quality checks, correction of image distortions caused by eddy currents and head motion, skull stripping, and calculation of diffusion metrics. Data quality checks are conducted by a radiologist with 10 years of extensive experience. Skull stripping is performed using the BET toolbox in FSL 5.0. Correction for eddy currents and head motion, as well as the calculation of diffusion metrics, are completed within the FMRIB Diffusion Toolbox in FSL 6.0.7.13 (following the latest protocols). Quality control is carried out through visual inspection and verification for outliers.

Network Construction

Nodes and edges are the two fundamental elements of a network. In this study, we constructed the WM structural network for each individual using definitions of network nodes, WM fiber imaging, and network edges. The brain was divided into 90 regions of interest (ROIs) according to the Automated Anatomical Labeling (AAL) 90 brain atlas, with each ROI defining a node in the network.²¹ The brain segmentation procedure was performed using the SPM12 software package. Deterministic fiber tractography was conducted using the Diffusion Toolkit software. Fiber tractography was initiated by identifying the principal diffusion direction in each voxel of the brain to obtain whole-brain fiber bundle imaging. Fiber tracking was stopped if the turning angle was greater than 45° or if the fractional anisotropy (FA) value was less than 0.2. To reduce the potential noise influence on the false connections generated by the whole-brain tractography, only WM connections between nodes are adopted when the fiber number (FN) is greater than 3. The edge weights (W_{ij}) are calculated as the product of FN and the average FA along the fiber bundle between the pair of interest regions, $W_{ij} = FN_{ij} \times FA_{ij}$. Based on the above steps, a 90×90 WM connectivity matrix was constructed for each subject.²⁰ The workflow for constructing the WM structural network is shown in [Figure 1](#).

Graph Theory Analysis

To better assess changes in brain networks, we analyze them from both global and nodal perspectives. Global parameters in this study mainly discuss: global efficiency, characteristic path length, clustering coefficient and small worldness, which also belong to small world attributes.²² Nodal parameters in this study focus on nodal efficiency and degree.²³ Based on the classification of nodal degree, three types of subnet connections can be identified: rich-club connections between rich club nodes (the top 15% of the nodal degrees in 90 brain regions), feeder connections between rich-club and non-rich club nodes, and local connections between non-rich club nodes.²⁴ The rich-club phenomenon serves as the basis for information integration and segregation in the human brain, emphasizing the role of core brain regions within the network. Feeder connections are responsible for transmitting information from non-rich club nodes to the rich club, establishing a hierarchical “local-to-global” transmission pathway. Local connections represent direct links between non-rich club nodes, maintaining basic connectivity in local regions.²⁵ The calculation methods for the three connection strengths are the average of all connections in their corresponding subnetworks. Detailed calculation methods and definitions for these parameters are provided in [Supplementary Table 1](#). All topological calculations were performed using the MATLAB toolbox “GRETNA” and visualized with the BrainNet Viewer toolbox.²⁶

Measurement of Inflammatory Factors

During the follow-up visit 1 month after injury, after fasting overnight, fasting blood samples (5 mL of venous blood) were collected in the morning without anticoagulation. The samples were allowed to sit naturally for 30 minutes and then centrifuged at 3000 revolutions per minute for 10 minutes. The supernatants were collected and stored at −20°C. ELISA was used to measure the levels of IL-8, IL-9, IL-10, IL-17A, MCP-1 and TNF-α according to the instructions provided in the ELISA kits. To minimize analytical variability, all samples were analyzed in duplicate on the same day in a random order by a technician blinded to the clinical diagnoses; the intra-assay coefficient of variation was <5%.²⁷

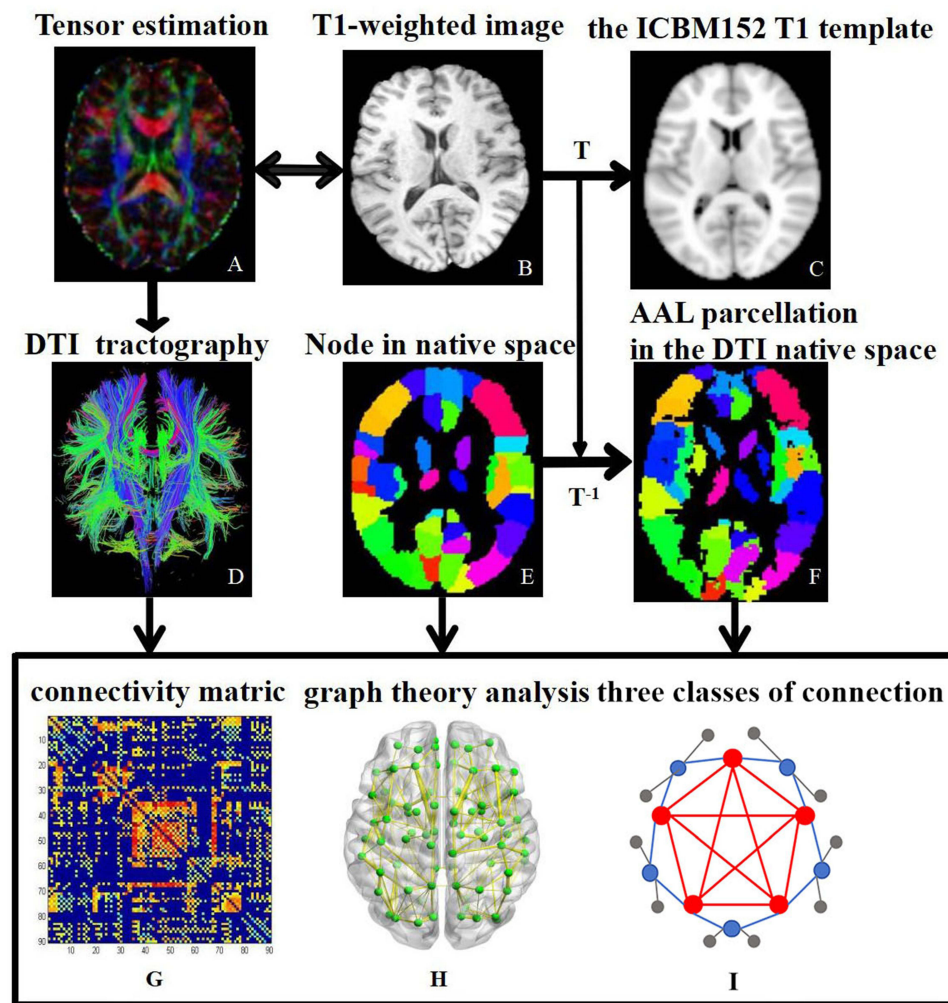


Figure 1 The flow chart. (A–F) Data process: Individual brain structural spatial registration was performed using T1-weighted images and the ICBM152 standard template, with preprocessing steps (eg, denoising, motion correction, brain region segmentation) to standardize structural data. Based on DTI tractography, white matter fiber connections were reconstructed within the individual's native space by setting seed points and applying deterministic tractography algorithms to extract fiber pathways between brain regions. To define network nodes, the AAL atlas was registered to the individual's DTI native space, with 90 brain regions designated as network nodes. (G) Individual brain structural connectivity matrix: An individualized structural connectivity matrix was constructed by quantifying the number of fiber connections between brain regions. In this matrix, rows and columns correspond to brain region nodes, and the matrix element values represent the connection strength between nodes. (H) The visualization of structural brain network: Based on graph theory analysis, the topological properties of the network are examined from both the network and node dimensions. Green node means one brain region, and yellow edge means possible connection between two brain regions. (I) Schematic diagram of the subnetwork connection model: The network is further subdivided into three hierarchical sub-networks—rich-club connection (red node and red edge), feeder connection (blue node and blue edge), and local connection (gray node and gray edge)—based on descending edge connection strength. This classification reveals the integration and segregation characteristics of the structural brain network.

Statistic Analysis

This study employed SPSS 27.0 data organization and analysis. The Shapiro–Wilk test and Levene's test were utilized to assess the normality and homogeneity of variance of the data, respectively. For measurement data that met the criteria for normal distribution and homogeneity of variance, statistical descriptions were presented as mean±standard deviation ($m \pm s$), and comparisons between two groups were conducted using the independent two-sample *t*-test. For count data, statistical analysis was performed using case counts, and differences were analyzed using the chi-square test. Prior to all difference analyses, relevant covariates were adjusted. When comparing multiple brain regions, the false discovery rate (FDR) was applied for correction. Risk factors for the occurrence of SD with 3 months after injury in patients with mTBI were screened through univariate and multivariate logistic regression analyses, and regression models were constructed based on these factors. The predictive performance of the models was evaluated using receiver operating characteristic (ROC) curves. Pearson correlation analysis was conducted to explore potential associations between indicators and PSQI scores. All tests were two-sided, and a p -value < 0.05 was considered statistically significant.

Results

Demographic and Clinical Characteristics

In the follow-up study of 232 participants with mild traumatic brain injury (mTBI), 17 subjects were excluded: 4 due to secondary injuries, 4 due to self-medication, 6 who were lost to follow-up, and 3 whose image showed the bad MRI data quality. Ultimately, data from 215 participants were collected. Among them, 130 participants (60.5%) experienced sleep disturbances at the end of the follow-up period (mTBI-ND group), while 85 participants (39.5%) were not diagnosed with sleep disturbances during the follow-up period (mTBI-SD group). Compared to the mTBI-ND group, the mTBI-SD group had a significantly higher proportion of males ($\chi^2=4.12$; $p=0.04$) and a significantly higher PSQI score 3 months after injury ($t=8.39$; $p<0.001$). The remaining clinical and demographic characteristics of the two groups are presented in Table 1.

Differences in the WM Network Between the mTBI-SD and mTBI-ND Groups

In the WM network topological analysis of DTI images one month after injury, significant differences in multiple topological properties were observed between the two mTBI groups after covariate adjustment. Among global properties, although no significant differences were found in global efficiency, characteristic path length, clustering coefficient or small-worldness (Supplementary Table 2), alterations in nodal properties were observed in specific brain regions. The

Table 1 Comparison of Demographic Data Between the mTBI-SD and mTBI-ND Groups

	mTBI-ND (n=85)	mTBI-SD (n=130)	p
Age (m±s)	41.52±16.82	42.31±13.43	0.80
Male (n,%)	35 (41.18)	83 (63.85)	0.04*
BMI (m±s)	20.85±3.52	20.61±2.41	0.68
Smoking (n,%)	50 (58.82)	75 (57.70)	0.91
Drinking (n,%)	38 (44.71)	55 (42.30)	0.92
Injury cause			
Traffic accident (n,%)	40 (47.06)	50 (38.46)	0.50
Fall (n,%)	5 (5.88)	10 (7.69)	
Violence/Assault (n,%)	25 (29.41)	50 (38.46)	
Others (n,%)	15 (17.64)	20 (15.38)	
CT positive symptom			
Skull fracture (n,%)	15 (17.65)	13 (10.00)	0.33
Hematoma (n,%)	5 (5.88)	8 (6.15)	
Contusion (n,%)	7 (8.24)	9 (6.92)	
No findings (n,%)	58 (68.24)	100 (76.92)	
GCS score			
15 (n,%)	58 (67.65)	95 (73.08)	0.63
14 (n,%)	24 (28.24)	30 (23.08)	
13 (n,%)	3 (2.94)	5 (3.85)	
Marshall CT classification			
I (n,%)	63 (74.12)	113 (86.54)	0.12
II (n,%)	22 (25.88)	17 (13.46)	
PSQI			
On admission	3.52±1.63	3.77±1.28	0.21
1 month after mTBI (m±s)	5.55±3.89	5.34±3.11	0.78
3 months after mTBI (m±s)	4.29±1.47	10.87±2.61	<0.01*

Notes: Values were displayed as mean ± standard deviation (m±s). P value of male, smoking, drinking, injury cause, CT positive symptom, GCS score and Marshall CT classification was calculated by chi-square test and p values of age, BMI and PSQI scores were obtained by independent-samples t test. p* means $p<0.05$.

Abbreviations: BMI, Body Mass Index; GCS score, Glasgow Coma Scale score; PSQI, Pittsburgh sleep quality index.

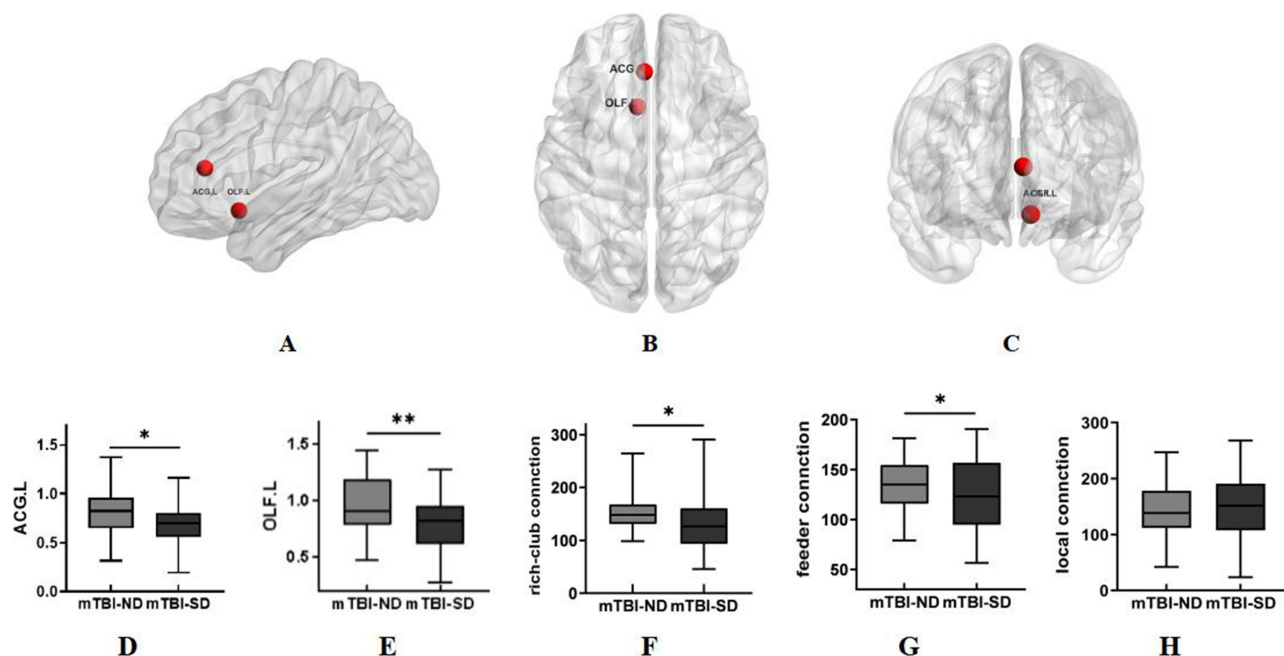


Figure 2 The differences between two mTBI groups. (A–C) Node schematic: the schematic shows the location of two brain regions, ACG.L and OLF.L respectively. (D–H) The box plot: Significant differences in the nodal efficiency of ACG.L and OLF.L and the connection strength of rich-club and feeder.

Notes: *means $p < 0.05$. **means $p < 0.01$.

Abbreviations: ACG.L, left anterior cingulate gyrus; OLF.L, left olfactory cortex.

mTBI-SD group exhibited significantly lower nodal efficiency in OLF.L ($t=3.10$, $p=0.003$) and ACG.L ($t=2.41$, $p=0.02$) compared to the mTBI-ND group (Figure 2A–E), while no significant differences were detected in nodal efficiency across other brain regions. Furthermore, in rich-club phenomenon, the mTBI-SD group demonstrated reduced rich-club connection strength ($t=2.29$, $p=0.02$) and feeder connection strength ($t=2.07$, $p=0.04$) relative to the mTBI-ND group (Figure 2F–H), whereas no significant difference was found in local connection strength.

Differences in Inflammatory Factors

As is shown in Table 2, in the detection of various inflammatory factors 1 month after injury, after adjusting for covariates, it was found that the levels of IL-8 ($t_{IL-8}=2.30$, $p=0.02$), IL-10 ($t_{IL-10}=2.31$, $p=0.02$), and TNF- α ($t_{TNF-\alpha}=3.82$, $p<0.01$) in the mTBI-SD group were significantly higher than those in the mTBI-ND group. No differences in other inflammatory factors were observed between the two groups.

Table 2 Differences in Inflammatory Factors

Inflammatory Factor (pg/mL)	mTBI-ND (n=85)	mTBI-SD (n=130)	p
IL-8	14.54 \pm 3.87	17.14 \pm 5.80	0.02*
IL-9	50.55 \pm 30.21	63.77 \pm 35.12	0.08
IL-10	20.80 \pm 10.03	25.80 \pm 9.68	0.02*
IL-17	14.17 \pm 3.98	16.15 \pm 5.80	0.09
MCP-I	10.71 \pm 5.98	12.78 \pm 6.44	0.14
TNF- α	4.22 \pm 2.08	3.19 \pm 1.68	<0.01*

Notes: P values were obtained by independent-samples t test. p^* means $p<0.05$.

Abbreviations: IL-8, Interleukin-8; IL-9, Interleukin-9; IL-10, Interleukin-10; IL-17, Interleukin-17; MCP-I, Monocyte chemoattractant protein-I; TNF- α , tumor necrosis factor.

Logistic Regression Analysis

Based on the above statistical difference analysis, we used the occurrence of SD 3 months after injury as the dependent variable, and the eight parameters (gender, IL-8, IL-10, TNF- α , OLF.L nodal efficiency, ACG.L nodal efficiency, rich-club connection strength, and feeder connection strength) as independent variables. After standardizing the data, they were included in the univariate and multivariate logistic regression model analysis. The results are shown in Table 3. Among them, IL-8, TNF- α , OLF.L, ACG.L, and rich-club connection strength are independent influencing factors of mTBI-SD, with regression coefficients of 1.79, 1.93, 0.62, 0.51, and 0.59, respectively. However, in the multivariate analysis, IL-8 and ACG.L nodal efficiency no longer retained their original significance.

The AUC of univariate and multivariate logistic regression models are shown in Table 4 and Figure 3. The inflammatory indicators exhibit high sensitivity, whereas the brain network parameters demonstrate high specificity. Among them, the individual parameter with the best discriminatory efficiency is TNF- α 1 month after injury (AUC=0.709), while the multi-parameter model of TNF- α , OLF.L, and rich-club connection 1 month after injury achieved the maximum predictive power (AUC=0.809). The sensitivity of this model is 74.62%, the specificity is 76.47%, the positive predictive value(PPV) is 82.91%, the negative predictive value(NPV) is 66.33%, and the accuracy is 75.35%.

Correlation Analysis

As shown in Figure 4, in the mTBI-SD group, TNF- α , OLF.L nodal efficiency, and rich-club connection were significantly correlated with PSQI scores 3 months after injury ($r_{\text{TNF-}\alpha}$ =0.538, $p<0.01$; $r_{\text{OLF.L}}$ =-0.461, $p<0.01$; $r_{\text{rich-club connection}}$ =-0.563, $p<0.01$), but not with PSQI scores 1 month after injury ($p_{\text{TNF-}\alpha}$ =0.23; $p_{\text{OLF.L}}$ =0.36; $p_{\text{rich-club connection}}$ =0.18).

Table 3 Logistic Regression Analysis

Variables	Univariate Analysis (Corrected)			Multivariate Analysis (Corrected)		
	OR (95% CI)	β	p	OR (95% CI)	β	p
Male	0.64 (0.41–1.0)	−0.45	0.64	–	–	–
IL-8	1.79 (1.10–2.90)	0.58	0.02*	1.34 (0.79–2.27)	0.29	0.27
IL-10	0.97 (0.92–1.02)	−0.03	0.34	–	–	–
TNF- α	1.93 (1.15–3.23)	0.66	0.01*	2.02 (1.04–3.91)	0.70	0.04*
Rich-club	0.59 (0.37–0.95)	−0.53	0.03*	0.48 (0.27–0.86)	−0.73	0.01*
Feeder	0.77 (0.49–1.20)	−0.26	0.25	–	–	–

Note: p* means $p<0.05$.
Abbreviations: OLF.L, nodal efficiency of left olfactory cortex; ACG.L, nodal efficiency of right anterior cingulate cortex; IL-8, Interleukin-8; IL-10, Interleukin-10; TNF- α , tumor necrosis factor.

Table 4 ROC Analysis of Different Models

	ROC-AUC	95% CI	Sensitivity	Specificity
IL-8	0.649	0.54–0.75	69.42	62.39
TNF- α	0.709	0.64–0.76	73.82	67.44
OLF.L	0.669	0.50–0.73	49.80	78.80
ACG.L	0.589	0.52–0.66	43.85	72.94
rich-club	0.672	0.56–0.69	50.00	76.50
TNF- α +OLF.L+rich-club	0.809	0.75–0.86	74.62	76.47

Note: p* means $p<0.05$.
Abbreviations: OLF.L, nodal efficiency of left olfactory cortex; ACG.L, nodal efficiency of right anterior cingulate cortex; IL-8, Interleukin-8; TNF- α , tumor necrosis factor- α ; ROC, receiver operating characteristic curve; AUC, Area Under Curve.

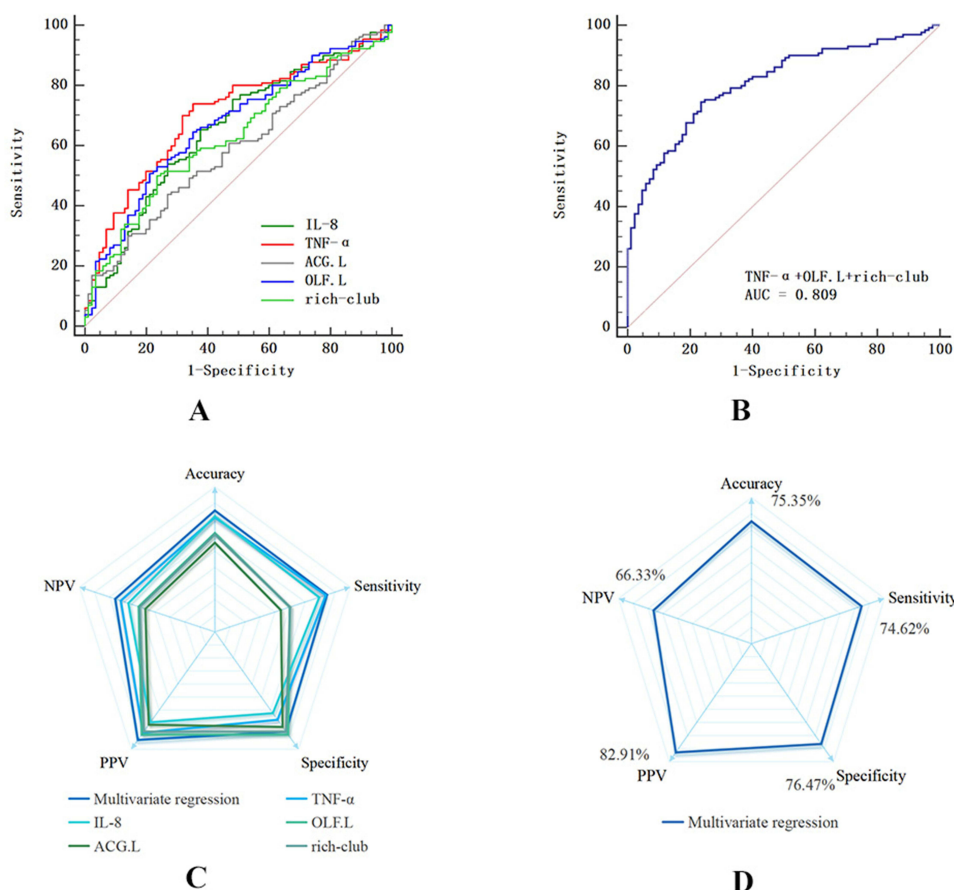


Figure 3 ROC curve analysis and some different features (**A** and **B**) The ROC curve of univariate and multivariate regression model. The multivariate regression model's ROC shows the greatest AUC(AUC=0.809). (**C** and **D**) Different features of ROCs. While taking the multivariate regression, the model has better comprehensive performance among others in prediction.

Abbreviations: OLF.L, nodal efficiency of left olfactory cortex; ACG.L, nodal efficiency of right anterior cingulate cortex; IL-8, Interleukin-8; TNF- α , tumor necrosis factor- α ; NPV, Negative Predictive Value.

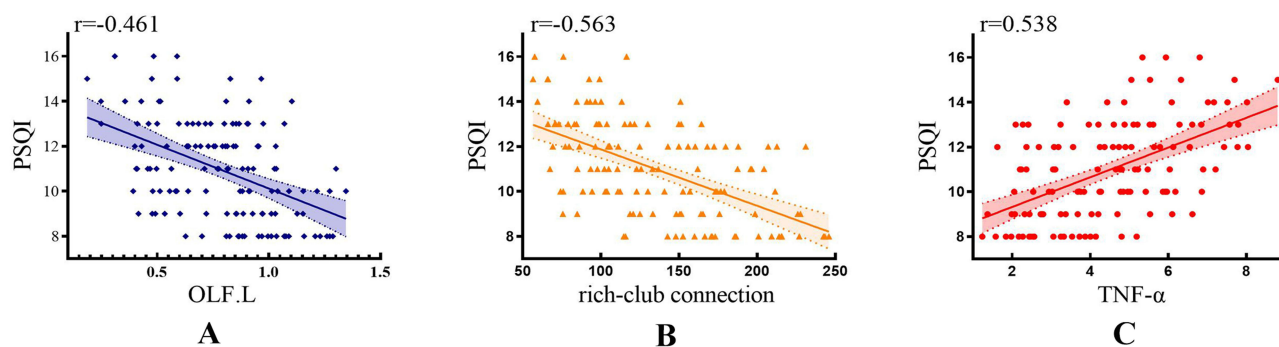


Figure 4 Pearson correlation analysis of PSQI with nodal efficiency of OLF.L (**A**), rich-club connection strength (**B**) and TNF- α (**C**) in mTBI-SD group.

Discussion

To our knowledge, this study is the first to attempt to link inflammatory factors and WM structural network topological properties to mTBI-SD, and to explore the relationship between inflammatory factors and WM topological properties and PSQI scores respectively. The main findings are as follows: 1) Patients with SD 3 months after mTBI exhibited differences in inflammatory factors and some indicators of brain networks compared to those without SD; 2) OLF.L, and rich-club connection strength and TNF- α were independent risk factors for SD 3 months after mTBI, and a combined

model effectively predicted the occurrence of SD at this time point; 3) OLF.L, rich-club connection strength, and TNF- α were significantly associated with PSQI scores 3 months after mTBI. By analyzing changes in inflammatory factors and WM topological properties 1 month after mTBI, this study is the first to construct a combined model of two biological indicators to predict the occurrence of mTBI-SD, providing a scientific clinical basis for early clinical prevention and treatment.

Previous studies have demonstrated that TNF- α , as a highly sensitive biological marker, possesses dual significant values: within a cross-sectional analysis framework, it enables early and precise quantitative assessment of the degree of neurodegenerative damage; in longitudinal follow-up studies, TNF- α , by activating the proinflammatory properties of microglia, effectively predicts the risk of developing late-onset related psychiatric disorders.^{28,29} As Masoum said, even without observable significant cortical damage, mTBI can trigger a series of complex neurobiological cascade reactions, leading to persistent neuroinflammation and thus forming a stubborn vicious cycle.¹⁶ Current mainstream theories generally agree that TNF- α exerts profound effects on the sleep cycle by acting on the neuroendocrine system and neurotransmitter levels.³⁰ According to Tahir Muhammad, in response to the potential metabolic homeostasis imbalance and dysfunction of nucleus pulposus cells induced by abnormally elevated TNF- α levels in mTBI patients, melatonin demonstrates a significant antagonistic effect on TNF- α -mediated metabolic abnormalities by activating the Akt / ERK / CREB signal transduction pathway.³¹ Existing research indicates that proinflammatory cytokines (such as TNF- α and IL-6) can accelerate the oxidative metabolism of melatonin in the liver by activating cytochrome P450 enzymes—particularly CYP1A2 and CYP2C19.³² Additionally, chronic inflammatory states may upregulate the activity of indoleamine 2,3-dioxygenase (IDO), promoting the diversion of tryptophan (a precursor of melatonin) toward the kynurenine pathway and indirectly reducing melatonin synthesis.³¹ This dual mechanism leads to decreased plasma melatonin levels and disrupts the regulation of the sleep-wake cycle.

Additionally, Ke Ding in a rat model of traumatic brain injury (TBI) has confirmed that melatonin, as an efficient free radical scavenger, exhibits remarkable antioxidant properties in mitigating the damage caused by oxidative stress to WM structures, thereby also demonstrating a significant protective effect on white matter damage induced by mTBI, with potential neuroprotective implications.³³ However, the persistent high-inflammatory state following mTBI significantly accelerates the clearance kinetics of melatonin in the body, resulting in a continuous decrease in plasma melatonin concentrations and thus maintaining a dynamic imbalance in sleep-related physiological regulatory pathways in the body.³⁴ A randomized controlled trial (RCT) by Grima et al in mTBI patients showed that 2 mg of melatonin supplementation before bedtime shortened sleep latency, though its effect on sleep maintenance was limited.³⁵ However, the safety of long-term melatonin use—such as potential hormonal interference—still requires further validation.

In above context, the brain region named OLF.L, which regulates melatonin secretion and receptor signaling, becomes particularly important. As a core area connecting the old and new cortices of the brain, the “rich club” (which means a network of highly connected brain regions) including OLF.L plays a crucial role.³⁴ The rich club represents efficient communication hubs within the entire brain network, and its high connection strength and the high cost associated with metabolic demands render the rich-club connection strength highly sensitive and specific in identifying abnormal network patterns.³⁶ Alessandra Griffa has revealed that, compared to healthy individuals, patients with sleep disorders exhibit a significant reduction in the rich-club connection strength in WM topological characteristics, indicating their inability to effectively balance excitatory and inhibitory signals transmitted by upstream nodes, thereby affecting the efficiency of sleep-related brain regions and their structural networks.³⁷ This finding further emphasizes the important roles of OLF.L, rich club connectivity strength and TNF- α in maintaining sleep homeostasis and brain network function, and provides new theoretical bases and research directions for precise interventions and effective treatments for sleep disorders following mTBI. In this study, we confirmed that OLF.L nodal efficiency, rich-club connection strength, and TNF- α levels in the mTBI-SD group were correlated with PSQI scores, further supporting the significant impact of these three indicators on SD 3 months after injury in mTBI patients. The combined prediction AUC of OLF.L nodal efficiency, rich-club connection strength, and TNF- α levels was 0.809, demonstrating clinical utility. Meanwhile, the multivariate logistic regression model exhibited more comprehensive evaluation effectiveness compared to every univariate models, potentially because the multivariate model better explains the occurrence of SD 3 months after injury from both inflammatory levels and WM structural networks, thus providing better performance value than every univariate one. This also suggests that comprehensively considering mTBI-related indicators can better predict the occurrence of SD.

It is noteworthy that, while studies with follow-up periods of six months or longer have also observed similar phenomena, the aforementioned results confirm that inflammatory and network topological indicators in the subacute phase are equally valuable for predicting the occurrence of mTBI-SD 3 months later, undoubtedly providing a more favorable basis for early disease diagnosis. Furthermore, in our study, no specific restrictions were placed on the location of mTBI lesions, suggesting that localized mTBI lesions may not be the direct cause of mTBI-SD. Perhaps the combined action of multiple biomarkers targeting different etiologies holds the key to unlocking the mystery of mTBI-SD. Limitations that should still be noted in the study include: 1) the lack of long-term follow-up data, which limits the understanding of the long-term evolutionary trends of mTBI; 2) the complex pathogenesis of mTBI-SD necessitates further refinement in the study of the role of inflammatory factors and brain networks; 3) the difficulty in sample collection due to the specificity of the patient population, particularly the neglect of asymptomatic patients, which can increase the difficulty of sample acquisition.

In summary, our study demonstrates that combining OLF.L nodal efficiency, rich-club connection strength, and TNF- α levels can objectively and effectively predict the occurrence of SD three months after mTBI, providing a more objective and effective method for predicting SD following mTBI. However, we also acknowledge that there is still much progress to be made. In future work, larger research samples are needed to validate our findings and optimize our model to better predict and intervene in sleep disorders among mTBI patients.

Conclusion

In summary, our research demonstrates that integrating the nodal efficiency of OLF.L, rich-club connection strength, and TNF- α levels can objectively and effectively predict the occurrence of SD in mTBI patients three months after injury. This approach offers a more objective and efficient method for predicting SD following mTBI. However, we acknowledge that there is still much progress to be made. In future work, larger research samples are needed to validate our findings and optimize our model, in order to better predict and intervene in SD among mTBI patients.

Abbreviations

TBI, traumatic brain injury; mTBI, mild traumatic brain injury; SD, sleeping disorders; ND, no sleeping disorders; MRI, magnetic resonance imaging; DTI, diffusion tensor imaging; WM, white matter; IL-8, interleukin-8; IL-9, interleukin-9; IL-10, interleukin-10; IL-17A, interleukin-17A; MCP-1, monocyte chemotactic protein-1; TNF- α , tumor necrosis factor; GCS, Glasgow Coma Scale; PSQI, Pittsburgh Sleep Quality Index; ELISA, Enzyme-linked immunosorbent assay; OLF.L, left olfactory cortex; ACG.L, left anterior cingulate and paracingulate gyri.

Data Sharing Statement

The data that support the findings of this study are available from the corresponding author, Subo Zhang upon reasonable request.

Ethics Statement

The study was conducted in accordance with the Declaration of Helsinki and approved by the Institutional Review Board of Zhenjiang First People's Hospital in Zhenjiang, China (Approval Number: KY20210926). Informed consent was obtained from all subjects involved in the study.

Acknowledgments

The authors thank all patients, their families, and the investigators who participated in this study. The authors also thank Dr. Li for his guidance of revising the manuscript.

Author Contributions

All authors made a significant contribution to the work reported, whether that is in the conception, study design, execution, acquisition of data, analysis and interpretation, or in all these areas; took part in drafting, revising or critically

reviewing the article; gave final approval of the version to be published; have agreed on the journal to which the article has been submitted; and agree to be accountable for all aspects of the work.

Funding

This work was supported by Key Project of Yangzhou Health Commission (2023-1-03) and Key Project of Gaoyou Science and Technology Bureau (GY20221201).

Supplementary Materials

[Supplement material 1.](#)

Disclosure

The authors report no conflicts of interest in this work.

References

1. Madhok DY, Rodriguez RM, Barber J, et al. TRACK-TBI investigators. outcomes in patients with mild traumatic brain injury without acute intracranial traumatic injury. *JAMA Network Open*. 2022;5(8):e2223245. PMID: 35976650; PMCID: PMC9386538. doi:10.1001/jamanetworkopen.2022.23245
2. Andrews MJ, Salat DH, Milberg WP, McGlinchey RE, Fortier CB. Poor sleep and decreased cortical thickness in veterans with mild traumatic brain injury and post-traumatic stress disorder. *Mil Med Res*. 2024;11(1):51. PMID: 39098930; PMCID: PMC11299360. doi:10.1186/s40779-024-00557-0
3. Freeman D, Sheaves B, Waite F, Harvey AG, Harrison PJ. Sleep disturbance and psychiatric disorders. *Lancet Psychiatry*. 2020;7(7):628–637. PMID: 32563308. doi:10.1016/S2215-0366(20)30136-X
4. Azeem A, Abdallah C, von Ellenrieder N, et al. Explaining slow seizure propagation with white matter tractography. *Brain*. 2024;147(10):3458–3470. doi:10.1093/brain/awae192
5. Mei Y, Qiu D, Xiong Z, et al. Disrupted topologic efficiency of white matter structural connectome in migraine: a graph-based connectomics study. *J Headache Pain*. 2024;25(1):204. doi:10.1186/s10194-024-01919-8
6. Dan XJ, Wang YW, Sun JY, et al. Reorganization of intrinsic functional connectivity in early-stage Parkinson's disease patients with probable REM sleep behavior disorder. *NPJ Parkinson's Dis*. 2024;10(1):5. PMID: 38172178; PMCID: PMC10764752. doi:10.1038/s41531-023-00617-7
7. Chen S, Wang SH, Bai YY, Zhang JW, Zhang HJ. Comparative study on topological properties of the whole-brain functional connectome in idiopathic rapid eye movement sleep behavior disorder and parkinson's disease without RBD. *Front Aging Neurosci*. 2022;14:820479. PMID: 35478699; PMCID: PMC9036484. doi:10.3389/fnagi.2022.820479
8. Peng J, Yang J, Li J, et al. Disrupted brain functional network topology in essential tremor patients with poor sleep quality. *Front Neurosci*. 2022;16:814745. PMID: 35360181; PMCID: PMC8960629. doi:10.3389/fnins.2022.814745
9. Chen G, Wang W, Wu H, et al. Disrupted topological properties of structural brain networks present a glutamatergic neuropathophysiology in people with narcolepsy. *Sleep*. 2024;47(6):zsae002. PMID: 38173348. doi:10.1093/sleep/zsae002
10. Zhu X, Ni K, Tan H, et al. Abnormal brain network topology during non-rapid eye movement sleep and its correlation with cognitive behavioral abnormalities in narcolepsy type 1. *Front Neurol*. 2021;11:617827. PMID: 33505350; PMCID: PMC7829333. doi:10.3389/fneur.2020.617827
11. Guedes VA, Kenney K, Shahim P, et al. CENC Multisite Observational Study Investigators. Exosomal neurofilament light: a prognostic biomarker for remote symptoms after mild traumatic brain injury? *Neurology*. 2020;94(23):e2412–e2423. PMID: 32461282; PMCID: PMC7455370. doi:10.1212/WNL.0000000000009577
12. Friberg S, Lindblad C, Zeiler FA, et al. Fluid biomarkers of chronic traumatic brain injury. *Nat Rev Neurol*. 2024;20(11):671–684. doi:10.1038/s41582-024-01024-z
13. To XV, Mohamed AZ, Cumming P, et al. Diffusion tensor imaging and plasma immunological biomarker panel in a rat traumatic brain injury (TBI) model and in human clinical TBI. *Front Immunol*. 2023;14:1293471. doi:10.3389/fimmu.2023.1293471
14. Green TRF, Carey SD, Mannino G, Craig JA, Rowe RK, Zielinski MR. Sleep, inflammation, and hemodynamics in rodent models of traumatic brain injury. *Front Neurosci*. 2024;18:1361014. PMID: 38426017; PMCID: PMC10903352. doi:10.3389/fnins.2024.1361014
15. Clarke GJB, Skandsen T, Zetterberg H, et al. Longitudinal associations between persistent post-concussion symptoms and blood biomarkers of inflammation and CNS-injury after mild traumatic brain injury. *J Neurotrauma*. 2024;41(7–8):862–878. PMID: 38117157. doi:10.1089/neu.2023.0419
16. Khosh-Fetrat M, Kosha F, Ansari-Moghaddam A, et al. Determining the value of early measurement of interleukin-10 in predicting the absence of brain lesions in CT scans of patients with mild traumatic brain injury. *J Neurol Sci*. 2023;446:120563. PMID: 36701890. doi:10.1016/j.jns.2023.120563
17. Ryan E, Kelly L, Stacey C, et al. Mild-to-severe traumatic brain injury in children: altered cytokines reflect severity. *J Neuroinflammation*. 2022;19(1):36. PMID: 35130911; PMCID: PMC8822689. doi:10.1186/s12974-022-02390-5
18. Yumul JN, Catroppa C, McKinlay A, Anderson V. Post-concussive symptoms in preschool children up to three months post-injury. *Dev Neurorehabil*. 2023;26(5):338–347. PMID: 37548355. doi:10.1080/17518423.2023.2242945
19. Djukic S, Phillips NL, Lah S. Sleep outcomes in pediatric mild traumatic brain injury: a systematic review and meta-analysis of prevalence and contributing factors. *Brain Inj*. 2022;36(12–14):1289–1322. PMID: 36413091. doi:10.1080/02699052.2022.2140198

20. Nelson LD, Temkin NR, Dikmen S, et al. Recovery after mild traumatic brain injury in patients presenting to US level I trauma centers: a transforming research and clinical knowledge in traumatic brain injury (TRACK-TBI) study. *JAMA Neurol.* **2019**;76(9):1049–1059. PMID: 31157856; PMCID: PMC6547159. doi:10.1001/jamaneurol.2019.1313
21. van den Heuvel MP, Sporns O. Rich-club organization of the human connectome. *J Neurosci.* **2011**;31(44):15775–15786. PMID: 22049421; PMCID: PMC6623027. doi:10.1523/JNEUROSCI.3539-11.2011
22. John M, Ikuta T, Ferbinteanu J. Graph analysis of structural brain networks in Alzheimer's disease: beyond small world properties. *Brain Struct Funct.* **2017**;222(2):923–942. PMID: 27357309. doi:10.1007/s00429-016-1255-4
23. Jiang W, Zhao Z, Wu Q, et al. Study on brain structure network of patients with delayed encephalopathy after carbon monoxide poisoning: based on diffusion tensor imaging. *Radiol Med.* **2021**;126(1):133–141. PMID: 32557108. doi:10.1007/s11547-020-01222-x
24. Peng L, Chen Z, Gao X. Altered rich-club organization of brain functional network in autism spectrum disorder. *Biofactors.* **2023**;49(3):612–619. PMID: 36785880. doi:10.1002/biof.1933
25. Whalley K. Neuronal networks: in the rich club. *Nat Rev Neurosci.* **2011**;13(1):3. PMID: 22108626. doi:10.1038/nrn3152
26. Wang J, Wang X, Xia M, Liao X, Evans A, He Y. GRETNA: a graph theoretical network analysis toolbox for imaging connectomics. *Front Hum Neurosci.* **2015**;9:386. PMID: 26175682; PMCID: PMC4485071. doi:10.3389/fnhum.2015.00386
27. Aisiku IP, Yamal JM, Doshi P, et al. Plasma cytokines IL-6, IL-8, and IL-10 are associated with the development of acute respiratory distress syndrome in patients with severe traumatic brain injury. *Crit Care.* **2016**;20(1):288. PMID: 27630085; PMCID: PMC5024454. doi:10.1186/s13054-016-1470-7
28. Frankola KA, Greig NH, Luo W, Tweedie D. Targeting TNF- α to elucidate and ameliorate neuroinflammation in neurodegenerative diseases. *CNS Neurol Disord Drug Targets.* **2011**;10(3):391–403. PMID: 21288189; PMCID: PMC4663975. doi:10.2174/187152711794653751
29. Probert L. TNF and its receptors in the CNS: the essential, the desirable and the deleterious effects. *Neuroscience.* **2015**;302:2–22. PMID: 26117714. doi:10.1016/j.neuroscience.2015.06.038
30. Besedovsky L, Lange T, Haack M. The sleep-immune crosstalk in health and disease. *Physiol Rev.* **2019**;99(3):1325–1380. PMID: 30920354; PMCID: PMC6689741. doi:10.1152/physrev.00010.2018
31. Muhammad T, Ali T, Ikram M, Khan A, Alam SI, Kim MO. Melatonin rescue oxidative stress-mediated neuroinflammation/ neurodegeneration and memory impairment in scopolamine-induced amnesia mice model. *J Neuroimmune Pharmacol.* **2019**;14(2):278–294. PMID: 30478761. doi:10.1007/s11481-018-9824-3
32. Ding S. Dynamic reactive astrocytes after focal ischemia. *Neural Regen Res.* **2014**;9(23):2048–2052. PMID: 25657720; PMCID: PMC4316467. doi:10.4103/1673-5374.147929
33. Ding K, Wang H, Xu J, Lu X, Zhang L, Zhu L. Melatonin reduced microglial activation and alleviated neuroinflammation induced neuron degeneration in experimental traumatic brain injury: possible involvement of mTOR pathway. *Neurochem Int.* **2014**;76:23–31. PMID: 24995391. doi:10.1016/j.neuint.2014.06.015
34. Won J, Alfini AJ, Smith JC. Cardiovascular endurance modifies the link between subjective sleep quality and entorhinal cortex thickness in younger adults. *Med Sci Sports Exerc.* **2021**;53(10):2131–2139. PMID: 33988545; PMCID: PMC8440339. doi:10.1249/MSS.0000000000002697
35. Grima NA, Rajaratnam SMW, Mansfield D, Sletten TL, Spitz G, Ponsford JL. Efficacy of melatonin for sleep disturbance following traumatic brain injury: a randomised controlled trial. *BMC Med.* **2018**;16(1):8. PMID: 29347988; PMCID: PMC5774131. doi:10.1186/s12916-017-0995-1
36. Chung AW, Mannix R, Feldman HA, Grant PE, Im K. Longitudinal structural connectomic and rich-club analysis in adolescent mTBI reveals persistent, distributed brain alterations acutely through to one year post-injury. *Sci Rep.* **2019**;9(1):18833. PMID: 31827105; PMCID: PMC6906376. doi:10.1038/s41598-019-54950-0
37. Griffa A, Van den Heuvel MP. Rich-club neurocircuitry: function, evolution, and vulnerability. *Dialogues Clin Neurosci.* **2018**;20(2):121–132. PMID: 30250389; PMCID: PMC6136122. doi:10.31887/DCNS.2018.20.2.agriffa
38. Barlow KM, Esser MJ, Veidt M, Boyd R. Melatonin as a treatment after traumatic brain injury: a systematic review and meta-analysis of the pre-clinical and clinical literature. *J Neurotrauma.* **2019**;36(4):523–537. PMID: 29901413. doi:10.1089/neu.2018.5752